

# Deformable liquid droplets for optical beam control

Hongwen Ren<sup>1,3</sup>, Su Xu<sup>2</sup>, and Shin-Tson Wu<sup>2,4</sup>

<sup>1</sup>Department of Polymer Nano-Science and Engineering, Chonbuk National University Jeonju, Jeonbuk, 561-756, Republic of Korea

<sup>2</sup>College of Optics and Photonics, University of Central Florida, Orlando, Florida 32816, USA

<sup>3</sup>hongwen@jbnu.ac.kr,

<sup>4</sup>swu@mail.ucf.edu

**Abstract:** We demonstrate a liquid droplet whose surface profile can be reshaped by voltage. As the dielectric force increases, the dome of a liquid droplet could touch the top substrate and become flat. While the voltage is removed, the droplet recovers to its original spherical shape. By choosing proper liquids, the required voltage for such a shape change is relatively low and the transition speed is fast. Potential application of such a deformable droplet for optical beam control is discussed.

©2010 Optical Society of America

**OCIS codes:** (010.1080) adaptive optics; (220.3630) lens; (230.2090) electro-optical devices

---

## References and links

1. N. A. Riza, and M. C. DeJule, "Three-terminal adaptive nematic liquid-crystal lens device," *Opt. Lett.* **19**(14), 1013–1015 (1994).
2. A. F. Naumov, G. D. Love, M. Yu. Loktev, and F. L. Vladimirov, "Control optimization of spherical modal liquid crystal lenses," *Opt. Express* **4**(9), 344–352 (1999).
3. V. V. Presnyakov, K. E. Asatryan, T. V. Galstian, and A. Tork, "Polymer-stabilized liquid crystal for tunable microlens applications," *Opt. Express* **10**(17), 865–870 (2002).
4. H. Ren, and S. T. Wu, "Adaptive liquid crystal lens with large focal length tunability," *Opt. Express* **14**(23), 11292–11298 (2006).
5. P. Valley, D. L. Mathine, M. R. Dodge, J. Schwiegerling, G. Peyman, and N. Peyghambarian, "Tunable-focus flat liquid-crystal diffractive lens," *Opt. Lett.* **35**(3), 336–338 (2010).
6. N. Chronis, G. L. Liu, K. H. Jeong, and L. P. Lee, "Tunable liquid-filled microlens array integrated with microfluidic network," *Opt. Express* **11**(19), 2370–2378 (2003).
7. H. Ren, and S. T. Wu, "Variable-focus liquid lens," *Opt. Express* **15**(10), 5931–5936 (2007).
8. S. H. Cho, F. S. Tsai, W. Qiao, N. H. Kim, and Y. H. Lo, "Fabrication of aspherical polymer lenses using a tunable liquid-filled mold," *Opt. Lett.* **34**(5), 605–607 (2009).
9. F. Schneider, J. Draheim, R. Kamberger, P. Waibel, and U. Wallrabe, "Optical characterization of adaptive fluidic silicone-membrane lenses," *Opt. Express* **17**(14), 11813–11821 (2009).
10. D. Zhu, C. Li, X. Zeng, and H. Jiang, "Tunable-focus microlens arrays on curved surfaces," *Appl. Phys. Lett.* **96**(8), 081111 (2010).
11. G. Beadie, M. L. Sandrock, M. J. Wiggins, R. S. Lepkowitz, J. S. Shirk, M. Ponting, Y. Yang, T. Kazmierczak, A. Hiltner, and E. Baer, "Tunable polymer lens," *Opt. Express* **16**(16), 11847–11857 (2008).
12. B. Berge, and J. Peseux, "Variable focus lens controlled by an external voltage: an application of electrowetting," *Eur. Phys. J. E* **3**(2), 159–163 (2000).
13. S. Grilli, L. Miccio, V. Vespini, A. Finizio, S. De Nicola, and P. Ferraro, "Liquid micro-lens array activated by selective electrowetting on lithium niobate substrates," *Opt. Express* **16**(11), 8084–8093 (2008).
14. T. Krupenkin, S. Yang, and P. Mach, "Tunable liquid microlens," *Appl. Phys. Lett.* **82**(3), 316–318 (2003).
15. S. Kuiper, and H. W. Hendriks, "Variable-focus liquid lens for miniature cameras," *Appl. Phys. Lett.* **85**(7), 1128–1130 (2004).
16. C. C. Cheng, C. A. Chang, and J. A. Yeh, "Variable focus dielectric liquid droplet lens," *Opt. Express* **14**(9), 4101–4106 (2006).
17. H. Ren, H. Xianyu, S. Xu, and S. T. Wu, "Adaptive dielectric liquid lens," *Opt. Express* **16**(19), 14954–14960 (2008).
18. H. Ren, D. Ren, and S. T. Wu, "A new method for fabricating high density and large aperture ratio liquid microlens array," *Opt. Express* **17**(26), 24183–24188 (2009).
19. S. Xu, Y. J. Lin, and S. T. Wu, "Dielectric liquid microlens with well-shaped electrode," *Opt. Express* **17**(13), 10499–10505 (2009).
20. H. Ren, S. H. Lee, and S. T. Wu, "Reconfigurable liquid crystal droplet using a dielectric force," *Appl. Phys. Lett.* **95**(24), 241108 (2009).
21. P. Penfield, and H. A. Haus, *Electrodynamics of Moving Media* (MIT, Cambridge, 1967).

## 1. Introduction

Adaptive liquid lenses based on molecular reorientation [1–5], pressure-induced liquid redistribution [6–9], thermal effect [10], polymer gel [11], electrowetting [12–15], and dielectrophoretic effect [16–19] have been studied extensively. These adaptive lenses have potential applications in image processing, machine vision, optical communication, and biomedical devices. Each type of lens has its own pros and cons. The lens based on dielectrophoretic effect (also called dielectric lens) is particularly attractive because of its simple structure, electrical actuation, large focal length tunability, fast response, and low power consumption. In a dielectric lens cell, two immiscible liquids with different dielectric constants are employed: one liquid forms a droplet on the bottom substrate and the other liquid fills the surrounding space. When a sufficiently high voltage is applied, the surface of the droplet can be reshaped by the generated dielectric force. Since the droplet behaves like a lens, its focal length can be tuned accordingly.

In a common dielectric liquid lens, the apex distance of the droplet is much smaller than the cell gap to prevent the dome of the droplet from touching the top substrate. If it touches the top substrate in a voltage-on state, the lens performance will be severely degraded and the droplet will no longer return to its original shape [20]. When such a droplet is used for beam control, the control ability is rather limited and the required voltage is very high.

In this paper, we demonstrate a liquid droplet whose dome can touch the top substrate and become flat under a relatively low voltage and, moreover, it returns to its initial state when the voltage is removed. We conducted experiments to prove our device concepts and analyzed the underlying physical mechanisms. Such a surface controllable droplet is useful for optical beam control. Furthermore, a droplet array with similar electro-optical properties can be used to make a large-panel optical switch.

## 2. Device structure and operation mechanism

Figure 1(a) shows the side-view structure of the droplet cell. Two immiscible liquids are sandwiched between two flat glass substrates: liquid-1 forms a droplet on the bottom substrate and liquid-2 fills the surrounding space. The inner surface of each glass substrate is first coated with indium tin oxide (ITO) electrode and then covered with a very thin dielectric layer. In the voltage-off state ( $V = 0$ ), the droplet is in relaxing state and its apex distance ( $t$ ) is smaller than the cell gap ( $t < d$ ). Such a structure is stable when the interfacial tension satisfies the following relation:

$$\gamma_{L-1,L-2} \cos \theta = \gamma_{L-1,D-1} - \gamma_{L-2,D-1}, \quad (1)$$

where  $\gamma$  is the interfacial tension and subscripts  $L-1$ ,  $L-2$ , and  $D-1$  represent liquid-1, liquid-2, and bottom dielectric layer, respectively, and  $\theta$  is the contact angle of the droplet. When a voltage is applied to the cell, the droplet surface bears an inhomogeneous electric field. The dielectric force exerted on the droplet can be expressed as [21]:

$$F_d = \frac{1}{2} \varepsilon_0 (\varepsilon_1 - \varepsilon_2) \nabla (E \cdot E), \quad (2)$$

where  $\varepsilon_0$ ,  $\varepsilon_1$ , and  $\varepsilon_2$  represent the permittivity of free space, liquid-1, and liquid-2, respectively, and  $E$  denotes the electric field on the curved droplet. If the applied voltage is high enough, the surface of the droplet can be reshaped adaptively in order to reach a new balanced state. If the condition of  $t \geq d$  is satisfied, the dome of the droplet will touch the top substrate surface, as shown in Fig. 1(b). The contact area of the dome depends on the size of the droplet. If the droplet is big, then the contact area will be large, as Fig. 1(c) shows. The shape of the droplet is fixed under a given voltage due to the balanced forces. However, this balance is broken and the shape of the droplet would adjust itself adaptively when the voltage is removed. If the droplet's surface tension is much larger than that of the top dielectric layer and liquid-2, the dielectric layer will not be strong enough to maintain the shape of the

droplet. The unbalanced surface tension will force the droplet to return to its original spherical shape, as Fig. 1(d) shows. The droplet switched between Fig. 1(d) and Fig. 1(c) can be used for beam control. At  $V = 0$ , an incident beam is highly diverged by the droplet because of the lens effect. While the dome becomes flat at  $V > 0$ , the beam will pass through the droplet without disturbance.

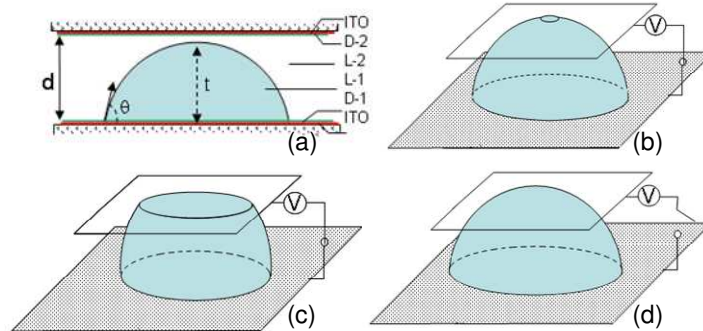


Fig. 1. Structure of the droplet cell and the operation mechanisms: (a) side-view structure at  $V = 0$ , (b) the dome of the droplet touching the top substrate surface with a voltage, (c) flat top surface, and (d) voltage is removed.

To briefly explain the shape change of the droplet from Fig. 1(c) to Fig. 1(d), we focus on the dome of the droplet touching the top dielectric layer, as shown in Fig. 2. If the dielectric constant of the droplet is larger than that of liquid-2, the generated dielectric force ( $F_d$ ) orients in outward direction. Such a force has horizontal and vertical components, but only the horizontal component ( $F_{dx}$ ) can deform the droplet. When the shape of the droplet is stabilized, the dielectric force and the interfacial tensions satisfy the following relationship:

$$\gamma_{L-1,D-2} = \gamma_{L-2,D-2} - \gamma_{L-1,L-2} \cos \phi + F_{dx}, \quad (3)$$

where  $\gamma_{L-1,D-2}$  and  $\gamma_{L-2,D-2}$  denote the interfacial tension of L-1/D-2 and L-2/D-2, respectively, and  $\phi$  is the contact angle of the droplet on the top substrate. If  $F_{dx}$  decreases,  $\phi$  will increase accordingly to reach a new balance, as depicted in Fig. 2. It means the contact area of the droplet has a tendency to shrink as the applied voltage decreases. From Eq. (3), if  $\gamma_{L-1,D-2} \gg \gamma_{L-2,D-2}$ , then removing the voltage ( $F_{dx} = 0$ ) would cause the angle  $\phi$  to be  $180^\circ$ . Under such a circumstance, the droplet will set apart from the top substrate and return to its original shape.

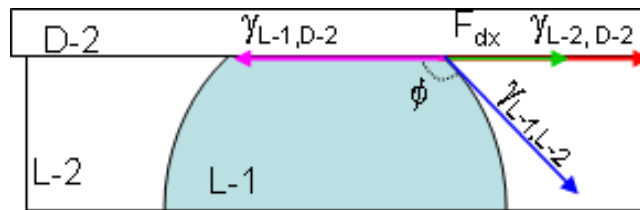


Fig. 2. Dielectric force and interfacial tensions for the balanced force analysis.

The droplet with its dome changed from Figs. 1(c) to 1(d) in voltage off state and from Figs. 1(d) to 1(c) in voltage-on state can be used for beam control. Figure 3 depicts its beam modulation in voltage-on and voltage-off states. Suppose the refractive index of L-1 is smaller than that of L-2 and the incident beam is collimated, then the spherical droplet can cause light to diverge, as shown in Fig. 3(a). When the dome of the droplet touches the substrate and becomes flat with large enough area in voltage on state, the light beam can pass through the droplet without disturbance, as shown in Fig. 3(b). The droplet can focus the beam if the

refractive index of L-1 is larger than that of L-2. At voltage off state, the optical power of the droplet is dependent on the size of the droplet and the refractive indices of the two materials.

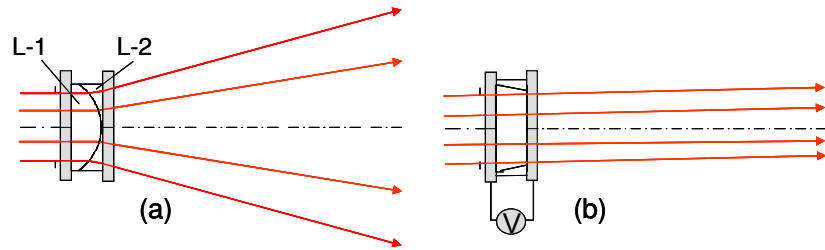


Fig. 3. The dome of the droplet with two different geometric shapes: (a) spherical shape in the voltage-off state, and (b) flat shape in a voltage-on state

### 3. Experimental realization

To demonstrate a liquid droplet which could indeed go through the shape changes as depicted in Fig. 1, we prepared a lens cell for experiments. Two ITO glass plates were chosen as the cell substrates. A very thin polyimide layer (PI2556, from HD Microsystems, surface tension  $\gamma_P \sim 40$  dynes/cm) was coated on the ITO electrodes. Glycerol (from Sigma-Aldrich) was chosen as L-1 and BK-7 matching liquid (from Cargille Labs) as L-2. At room temperature ( $\sim 23^\circ\text{C}$ ), the dielectric constant, refractive index, and surface tension of the glycerol are 47, 1.47, and  $\sim 63$  dyne/cm, respectively, and those of BK-7 matching liquid are 5, 1.52, and  $\sim 40$  dyne/cm, respectively. These two liquids are colorless and immiscible. To form droplets, we first mixed a small amount of glycerol with solvent ethanol. The solvent not only decreases the surface tension of the glycerol, but also dilutes the glycerol concentration in the mixture. When a small amount of this mixture was dripped on one substrate surface, the solvent was evaporated quickly, and various glycerol droplets on the substrate surface were obtained. After that, BK-7 matching liquid was used to cover all the droplets. The cell gap controlled by the spacers was  $\sim 50 \mu\text{m}$ .

### 4. Results and discussion

Various glycerol droplets were observed through an optical microscope. Due to the large surface tension, the aperture of each glycerol droplet exhibits a highly circular shape. Here, the droplet aperture is defined as the diameter of the droplet contacting the substrate surface. According to the droplet size, we classified them into three types: 1) the droplet that touches both substrates because of its large size, 2) the droplet presents a spherical shape, but its dome is close to the top substrate, and 3) the droplet whose apex distance is much smaller than the cell gap. Figure 4(a) shows four droplets with different sizes, as numbered from 1 to 4 in the descending order of aperture. The photo was taken by focusing on the surfaces of the droplets. Different from the other droplets, droplet-1 presents two clear rings, which implies that it contacts with both substrates at  $V = 0$ , as sketched in Fig. 1(c).

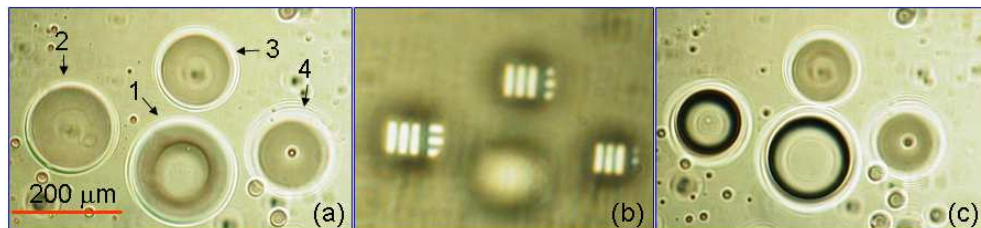


Fig. 4. Glycerol liquid droplets observed through an optical microscope: (a) focusing on droplet surfaces, (b) their imaging performance, and (c) focusing on the droplet surfaces at  $15 V_{\text{rms}}$

To confirm the shape of each droplet, we observed their imaging properties. A resolution target bar was placed under the cell as an object. By adjusting the distance between the object and the droplets, we could not get a clear image through droplet-1. The two rings [Fig. 4(a)] and blurry image [Fig. 4(b)] of droplet-1 indicate the droplet's dome is flattened by the top substrate. Meanwhile, clear bar images were observed through the other three droplets, although the images were slightly defocused as Fig. 4(b) shows. These clear images imply that the droplet surfaces are in spherical shape. At  $V = 16 V_{\text{rms}}$ , the surfaces of droplet-1 and droplet-2 are severely deformed [Fig. 4(c)]. Because the initial shape of droplet-2 is spherical at  $V = 0$ , we studied the dynamics of shape change in droplet-2. The aperture of droplet-2 was  $\sim 150 \mu\text{m}$  and its focal length was measured to be  $-1850 \mu\text{m}$  at  $V = 0$ . This droplet exhibits a negative optical power because the refractive index of the droplet ( $\sim 1.47$ ) is smaller than that of the surrounding liquid L-2 ( $\sim 1.52$ ). The apex distance of droplet-2 was calculated to be  $\sim 40 \mu\text{m}$ . That means the dome of droplet-2 is near to the top substrate because the cell gap is  $\sim 50 \mu\text{m}$ .

To track the deformed surface of droplet-2, we magnified the image size of droplet-2. At  $V = 0$ , we focused on the surface of the droplet, as shown in Fig. 5(a). The droplet is highly circular and has a clear border with its surrounded liquid. At  $V \sim 16 V_{\text{rms}}$  the surface of the droplet was deformed and its dome touched the top substrate [Fig. 5(b)]. This case corresponds to the droplet sketched in Fig. 1(b). As the voltage was increased to  $30 V_{\text{rms}}$ , the contact area on the top substrate expanded, as Fig. 5(c) shows. The droplet had two borders and the droplet profile between these two borders was observed. Such a shape corresponds to the one sketched in Fig. 1(c). As the voltage was decreased, the contact area of the droplet shrank accordingly. Finally, the droplet returned to its original spherical shape if the voltage was removed completely.

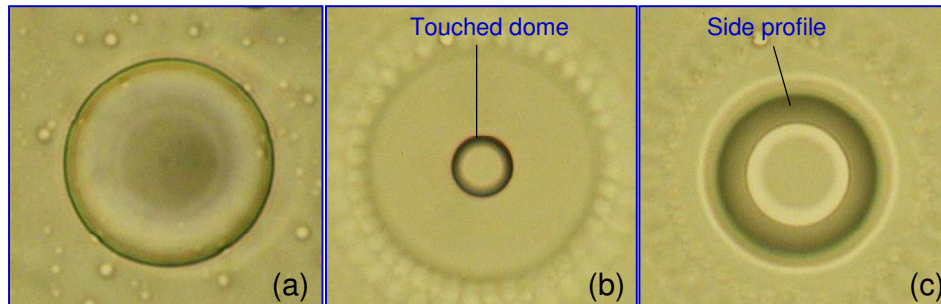


Fig. 5. The 2D images on the surface of droplet-2: (a)  $V = 0$ , (b)  $V = 16 V_{\text{rms}}$ , and (c)  $V = 30 V_{\text{rms}}$ .

Due to the large surface deformation of droplet-2, its electro-optical property should be different from other droplets. To measure its electro-optical property, the cell was placed in vertical direction and a collimated He-Ne laser was used as probing beam at normal incidence. The beam passing through a droplet was first expanded and then received by a photodiode detector. A diaphragm was placed in front of the detector. We adjusted the aperture of the diaphragm so that the detector could get the maximal intensity at  $V = 0$ . When a voltage was applied to droplet-2, the beam was adjusted by the droplet because of its surface profile change. Figure 6 depicts the voltage-dependent light intensity variation. As  $V$  increases to  $8 V_{\text{rms}}$ , the detected laser intensity starts to decrease. At  $V = 16 V_{\text{rms}}$ , the beam intensity reaches a minimum because the shape of the droplet shrinks and the outgoing beam diverges. When the voltage is further increased, the intensity increases because the dome of the droplet reaches the top substrate and forms a contact area; a portion of the incident beam passes through the area directly resulting in increased intensity. As the voltage gets higher than  $\sim 30 V_{\text{rms}}$ , the intensity gradually saturates. It implies that the shape of the droplet is not deformed further by the dielectric force, due to the surface tension of the droplet.

For comparison, we also measured the voltage-dependent light intensity through droplet-3, as shown in Fig. 6. As the applied voltage gets higher than  $20V_{\text{rms}}$ , the surface of droplet-3 begins to reshape and the transmitted light intensity declines gradually. Even at high voltages, no abrupt intensity change occurs. This result implies that its apex distance is much shorter than the cell gap and its dome does not touch the top substrate.

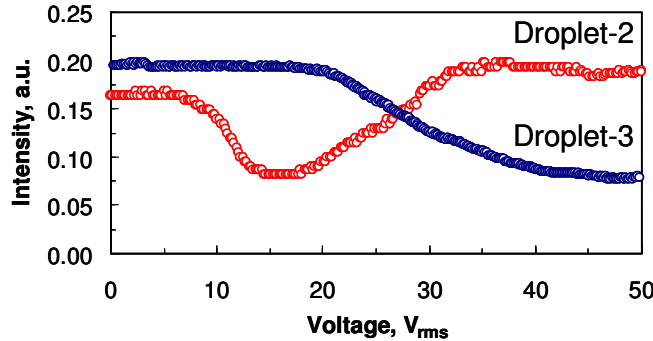


Fig. 6. Measured voltage-dependent transmittance of droplet-2 and droplet-3.

For beam control, response time is an important parameter. To measure the response time of droplet-2, we applied a gated square-wave of  $50 V_{\text{rms}}$  pulse to the cell. The light intensity change through the droplet-2 was recorded by a digital oscilloscope, as shown in Fig. 7. The cycle driving with two periods shows that the droplet returns to its original state very well. The rise and decay times were measured to be  $\sim 120$  ms and  $\sim 180$  ms, respectively. In the rising period, the droplet touches the top substrate in  $\sim 5$  ms. The rise time depends on the generated dielectric force while decay time depends on the interfacial surface tension and viscosity of the employed materials.

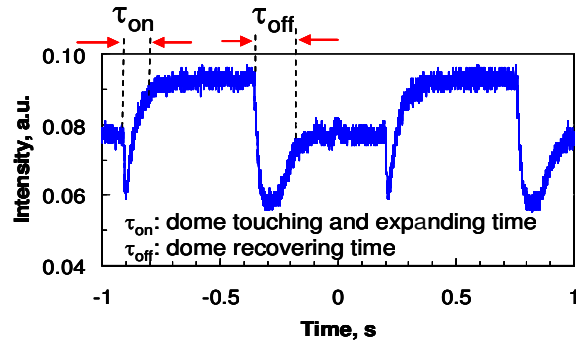


Fig. 7. Measured light intensity change of droplet-2 with time in two cycles.

To visually observe the various states of the droplets, we recorded a movie for tuning two droplets, as shown in Fig. 8. The apertures of these two droplets are  $\sim 170 \mu\text{m}$  and  $\sim 260 \mu\text{m}$ , respectively. In the voltage-off state, when focused on the surface of the droplets, each droplet had a dark border. The bigger droplet is in contact with both substrates because of its large size. For the smaller droplet, its dome is quite close to the top substrate but still keeps a spherical shape. The applied voltage is from 0 to  $\sim 20 V_{\text{rms}}$ . When the voltage increased, the bigger droplet was actuated first, but did not present any abrupt shape change. The smaller droplet suffered an abrupt shape change. As the voltage vanished, both droplets returned to their original shapes. From the video, we can see that the dome of the smaller droplet touches the top substrate at a fairly fast speed, and in each driving period the droplet returns to its original state.

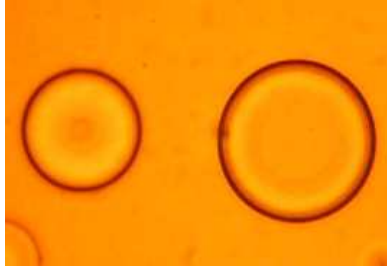


Fig. 8. Dynamic driving of two different droplets (Media 1).

Based on the above mentioned cell structure, we can increase the droplet size and make its dome close to the top substrate if the cell gap is thick enough. Usually a single liquid droplet is too small for practical applications. For a large size beam control or optical switch, it is possible to fabricate a liquid droplet array using cavity patterned method [18]. By controlling the shape of the droplet, the total aperture ratio of the droplet array can be increased significantly. By choosing proper liquids with a large refractive-index mismatch, the droplet will exhibit strong light scattering and divergence in the voltage-off state. However, in the voltage-on state the beam will transmit through in the regions where the dome touches the top substrate. Therefore, such a droplet can be used as optical beam control, especially for light-emitting diode (LED) beam modulation. For example in Fig. 3, we suppose the beam is from an LED, the beam can be expanded or collimated depending on the shape of the droplet. For a large-sized light switch, we can adopt a droplet array with the same electro-optical performance as that of droplet-2. To improve device stability and transition speed, it is desirable to coat polymers with quite different surface tensions on the two substrates. Although the density of L-1 ( $1.26 \text{ g/cm}^3$ ) is slightly smaller than that of L-2 ( $1.33 \text{ g/cm}^3$ ), the gravity effect will not be significant when the cell is placed in vertical position, because of the support from surface anchoring of substrates, surrounding L-2, and interfacial tension of the two liquids.

## 5. Conclusion

We investigated a liquid droplet whose dome is initially spherical but flattened by the top substrate as the voltage increases. If the dome of the droplet is close to the top substrate, the required voltage to deform the droplet is low ( $16 \text{ V}_{\text{rms}}$ ). The speed for the dome to touch the top substrate is fast ( $\sim 5 \text{ ms}$ ). Due to the reversible change between spherical and flat shapes, the droplet can be used for optical beam control. Potential application for a large-size optical switch using a droplet array is also discussed.